Volume 7

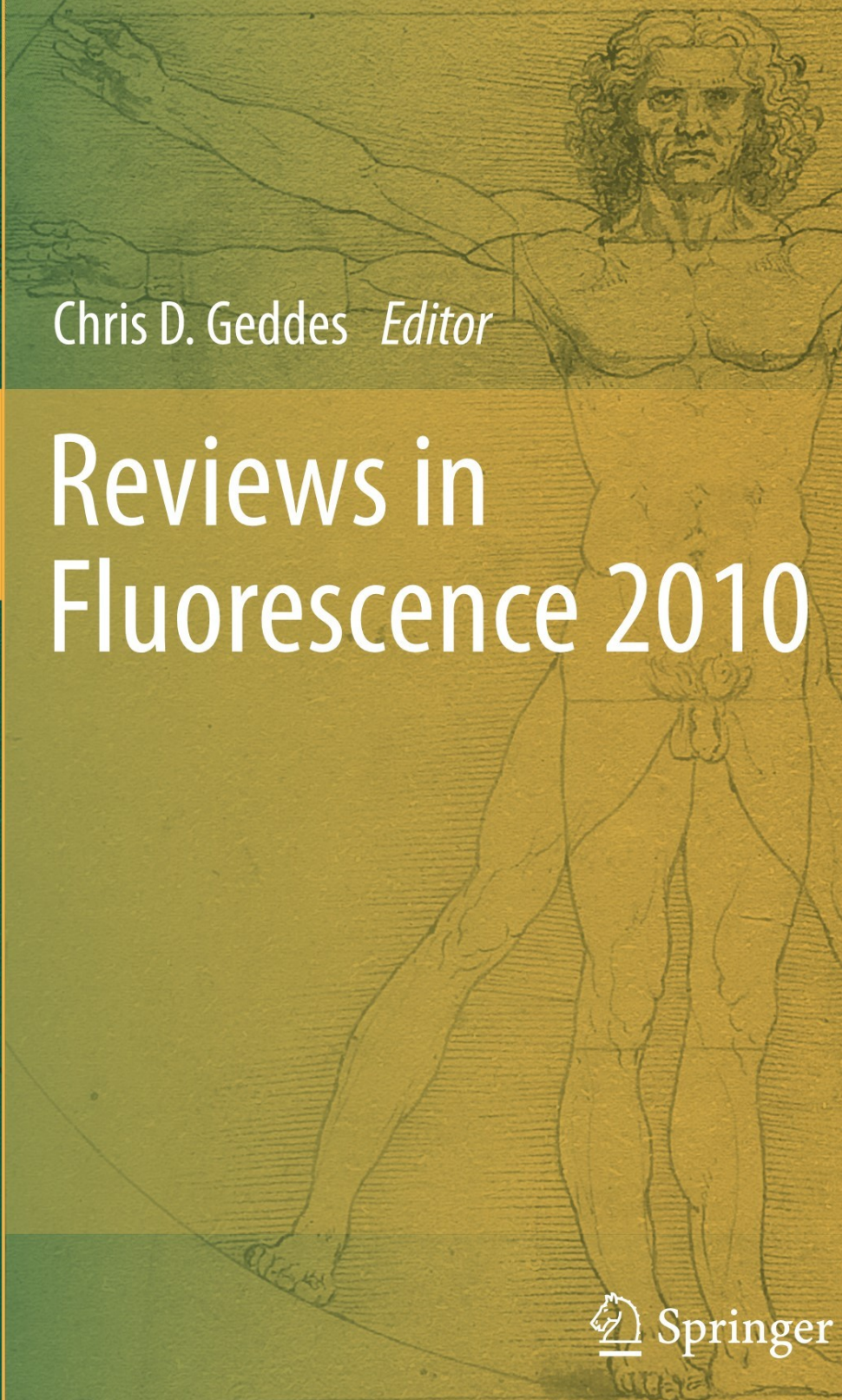

Chris D. Geddes *Editor*

Reviews in Fluorescence 2010

Springer

Reviews in Fluorescence

Editor
Chris D. Geddes

For further volumes:
http://www.springer.com/series/6946

Chris D. Geddes
Editor

Reviews in Fluorescence 2010

Springer

Editor
Chris D. Geddes
Institute of Fluorescence
University of Maryland
Baltimore, MD, 21202, USA
geddes@umbc.edu

Joseph R. Lakowicz
Center for Fluorescence Spectroscopy
725 Lombar Street
Baltimore, MD 21201
USA

ISSN 1573-8086
ISBN 978-1-4419-9827-9 e-ISBN 978-1-4419-9828-6
DOI 10.1007/978-1-4419-9828-6
Springer New York Dordrecht Heidelberg London

Library of Congress Control Number: 2011939299

Preface

This is the seventh volume in the popular fluorescence series, *Reviews in Fluorescence*. To date, six volumes have been both published and well received by the scientific community.

In this volume, we are pleased again with the broad and timely fluorescence content. We subsequently thank the authors for their very timely and exciting contributions again this year. We hope you will find this volume as useful as past volumes.

In closing, I would like to thank Caroleann Aitken, The Institute of Fluorescence manager, for help in coordinating content with authors and Michael Weston at Springer for help in publishing this current volume, thank you all.

Baltimore, MD, USA — Professor Chris D. Geddes

Contents

Contributors

Juan Baselga Departamento de Ciencia e Ingeniería de Materiales e Ingeniería Química, Universidad Carlos III de Madrid, Leganés, Madrid, Spain

Claire M. Brown McGill University Life Sciences Complex Imaging Facility, Montreal, QC, Canada

Juan C. Cabanelas Departamento de Ciencia e Ingeniería de Materiales e Ingeniería Química, Universidad Carlos III de Madrid, Leganés, Madrid, Spain

Ching-Wei Chang Department of Biomedical Engineering, University of Michigan, Ann Arbor, MI, USA

Amitabha Chattopadhyay Centre for Cellular and Molecular Biology, Council of Scientific and Industrial Research, Hyderabad, India

Michael P Coogan Department of Chemistry, Cardiff University, Wales, UK

David T. Cramb Department of Chemistry, University of Calgary, Calgary, AB, Canada

Marcelo H. Gehlen Instituto de Química de São Carlos, Universidade de São Paulo, São Carlos, SP, Brazil

Dixie J. Goss Chemistry Department, Hunter College, City University of New York, New York, NY, USA

Karl Otto Greulich Leibniz Institute of Age Research, Jena, Germany

Paulius Grigaravicius Leibniz Institute of Age Research, Jena, Germany

German Cancer Research Center, Heidelberg, Germany

Sourav Haldar Centre for Cellular and Molecular Biology, Council of Scientific and Industrial Research, Hyderabad, India

Ahmed A. Heikal Department of Chemistry and Biochemistry, Swenson College of Science and Engineering, The University of Minnesota Duluth, Duluth, MN, USA

Department of Pharmacy Practice and Pharmaceutical Sciences, College of Pharmacy, The University of Minnesota Duluth, Duluth, MN, USA

Hannah Ihms Department of Chemistry, University of Illinois at Urbana-Champaign, Urbana, IL, USA

Judith Lacoste MIA Cellavie Inc, Montreal, QC, Canada

Department of Biology, Cell Imaging and Analysis Network, McGill University, Montreal, QC, Canada

Robert P. Learmonth Department of Biological and Physical Sciences, Centre for Systems Biology, University of Southern Queensland, Toowoomba, QLD, Australia

Yao-Qun Li Department of Chemistry and Key Laboratory of Analytical Sciences, College of Chemistry and Chemical Engineering, Xiamen University, Xiamen, China

Xiu-Ying Li Department of Chemistry and Key Laboratory of Analytical Sciences, College of Chemistry and Chemical Engineering, Xiamen University, Xiamen, China

Na Li Department of Chemistry and Key Laboratory of Analytical Sciences, College of Chemistry and Chemical Engineering, Xiamen University, Xiamen, China

Li-Rong Lin Department of Chemistry and Key Laboratory of Analytical Sciences, College of Chemistry and Chemical Engineering, Xiamen University, Xiamen, China

Qian Liu Department of Chemistry and Key Laboratory of Analytical Sciences, College of Chemistry and Chemical Engineering, Xiamen University, Xiamen, China

David Lloyd Department of Microbiology, Cardiff Schools of Bioscience, Cardiff University, Wales, UK

Yi Lu Department of Chemistry, University of Illinois at Urbana-Champaign, Urbana, IL, USA

Olga Martín Departamento de Ciencia e Ingeniería de Materiales e Ingeniería Química, Universidad Carlos III de Madrid, Leganés, Madrid, Spain

Shamci Monajembashi Leibniz Institute of Age Research, Jena, Germany

Mary-Ann Mycek Department of Biomedical Engineering, University of Michigan, Ann Arbor, MI, USA

Trinh T. Nguyen Department of Chemistry, University of Calgary, Calgary, AB, Canada

Robson V. Pereira Instituto de Química de São Carlos, Universidade de São Paulo, São Carlos, SP, Brazil

Inés Piérola Departamento de Ciencia e Ingeniería de Materiales e Ingeniería Química, Universidad Carlos III de Madrid, Leganés, Madrid, Spain

Simon J A Pope Department of Chemistry, Cardiff University, Wales, UK

Javier Pozuelo Departamento de Ciencia e Ingeniería de Materiales e Ingeniería Química, Universidad Carlos III de Madrid, Leganés, Madrid, Spain

Carolina A. Sabatini Instituto de Química de São Carlos, Universidade de São Paulo, São Carlos, SP, Brazil

Berna Serrano Departamento de Ciencia e Ingeniería de Materiales e Ingeniería Química, Universidad Carlos III de Madrid, Leganés, Madrid, Spain

Ali Abbas Falih Shindi Department of Chemistry and Key Laboratory of Analytical Sciences, College of Chemistry and Chemical Engineering, Xiamen University, Xiamen, China

Emanuelle R. Simas Instituto de Química de São Carlos, Universidade de São Paulo, São Carlos, SP, Brazil

Aleksandrs Spurmanis McGill University Life Sciences Complex Imaging Facility, Montreal, QC, Canada

Jody L. Swift Department of Chemistry, University of Calgary, Calgary, AB, Canada

Charles Vining Department of Physiology, McGill University, Montreal, QC, Canada

Yu Xiang Department of Chemistry, University of Illinois at Urbana-Champaign, Urbana, IL, USA

Weichen Xu Department of Chemistry, University of Illinois at Urbana-Champaign, Urbana, IL, USA

Zhe-Xiang Zou Department of Chemistry and Key Laboratory of Analytical Sciences, College of Chemistry and Chemical Engineering, Xiamen University, Xiamen, China

Dongmei Zuo Goodman Cancer Centre, McGill University, Montreal, QC, Canada

How Does Tobacco Etch Viral mRNA Get Translated? A Fluorescence Study of Competition, Stability and Kinetics

Dixie J. Goss

Abstract Fluorescence techniques have been used to describe protein-protein and protein-nucleic acid interactions that lead to a competitive advantage for translation of tobacco etch viral mRNA. Using both quenching of intrinsic protein fluorescence and labeling of RNA, equilibrium and thermodynamic parameters were determined to gain insight into preferential binding of protein synthesis initiation factors (eIFs) to tobacco etch virus (TEV) mRNA and the mechanism of binding. Equilibrium data showed that the eIF4F complex binding to TEV mRNA was enthalpically favored and that the complex binds to TEV with greater stability than the cap complex. Kinetic studies using changes in fluorescence anisotropy further characterized the eIF4F-RNA interaction as a bi-molecular, single-step reaction. However, ionic strength dependence of the reaction revealed a possible conformational change after initial binding. These studies provide insight into how viral RNA can successfully compete with host cell mRNA through increasing stability of complexes and kinetic competition.

1 Introduction

This article is not intended to be an extensive review of viral translation, but rather describes the use of fluorescence to gain an increased understanding of a model system, described below. These fluorescence techniques are applicable to other protein assemblies and protein–nucleic acid interactions. A more complete description of viral RNA translation is reviewed in [1]. We have used equilibrium binding and kinetics as well as thermodynamic parameters to gain insight into preferential binding of protein synthesis initiation factors (eIFs) to tobacco etch virus (TEV) mRNA

D.J. Goss (✉)
Chemistry Department, Hunter College, City University of New York, 695 Park Ave, New York, NY 10065, USA
e-mail: dgoss@hunter.cuny.edu

C.D. Geddes (ed.), *Reviews in Fluorescence 2010*,
Reviews in Fluorescence, DOI 10.1007/978-1-4419-9828-6_1,

and the mechanism of binding. Viral RNA can compete with host cell RNA either through increasing the stability of complexes or through kinetic competition or both. We describe here our studies of the TEV internal ribosome entry site (IRES) RNA interactions with plant protein synthesis initiation factors.

Virtually all eukaryotic mRNAs possess a 5′ cap (m^7GpppN, where N is any nucleotide), a coding region and a poly A tail. During translation initiation, the 40S ribosome binds to an mRNA, scans to the initiation codon where it joins with the 60S subunit to form an 80S complex. This complex then proceeds to translate the coding region (for reviews see [2, 3]). Each of these steps requires the assistance of initiation factors (eIFs). Prior to 40S binding, eIF4E (the small subunit of eIF4F) binds to the cap at the 5′ terminus of RNA. eIF4G (the large subunit of eIF4F) binds and recruits additional eIFs including eIF4A, which is required to remove secondary structure in the noncoding region that would inhibit scanning of the 40S subunit. eIF3 promotes 40S ribosomal binding to the mRNA, and the poly A binding protein (PABP) stabilizes eIF4F binding to the cap. The poly A tail is the binding site for PABP. The interactions between PABP and eIF4G or eIF4B increase the poly A binding activity of PABP by tenfold and increase the affinity of eIF4F for the 5′ cap by 40-fold [4, 5]. However, there are numerous exceptions to this general description of translation initiation such as pausing or frameshifting. A major deviation from the classical model involves those RNAs, usually viral, that lack a cap structure altogether. These mRNAs possess a structured, non-coding region of 5′ RNA known as an internal ribosome entry site (IRES). Interestingly, IRESs are also beginning to be identified in cellular RNA [6]. These cellular mRNAs are generally those that would be advantageous to have translated under conditions where overall translation is compromised, for example mRNA coding for factors controlling growth or differentiation. As stated in one recent review [7] "the mechanism of IRES function remains essentially a black box."

Which mRNA then gets translated? Translation of mRNA in the eukaryotic cell is an extremely competitive process, and initiation, which is the rate-limiting step, is frequently where precise control is exercised. Viruses are presented with a particular problem in this regard. The initial step in gene expression of a virus in an infected cell is protein synthesis. However, upon entry into the eukaryotic cell, the viral RNA must successfully compete with the plethora of endogenous cellular mRNAs to ensure its own translation. In many cases a single viral RNA molecule is sufficient to ensure a productive infection. Most viruses actively shut off or greatly reduce host cell protein synthesis by disruption of some component of the translation apparatus. This strategy implies that the viral mRNA has some structural features that allow it to be distinguished from host mRNAs and to be translated by the modified host cellular machinery.

The 5′ untranslated region (UTR) of the viral mRNA is sufficient to confer its cap-independent translation in an in vitro system [8–12]. We have chosen as a model system the 5′ UTR of TEV for several reasons (1) TEV has a shorter noncoding 5′ sequence (143 nt) compared to a number of other viruses such as poliovirus (690 nt) (reviewed in [7, 13]) making it much easier to obtain quantities necessary for biophysical studies. (2) TEV has a poly A tail [12], unlike many other viruses that have some secondary or other structure in the 3′ region. We have quantitative data for

interactions of poly A and PABP and other eIFs. (3) TEV translational initiation factor requirements are relatively well characterized [14, 15]. (4) Most importantly, detailed chemical probing and mutations of the TEV sequence have identified critical regions necessary for translation [16]. A number of recent reviews [7, 17, 18] have been written about the general process of viral translation and the factors involved. We will describe here only recent information about TEV and other viruses similar to TEV. The picornaviral superfamily falls into the class of viruses that lack a 5′ cap structure. This family of viruses includes encephalomyocarditis virus, poliovirus and the plant virus, TEV among others. These viruses are very similar in that the positive-sense single-stranded RNA genome functions as a monocistronic mRNA. The mRNA codes for a single polyprotein, which is subsequently processed to form essential capsid and noncapsid proteins. These viral RNAs lack a 5′ cap and the 5′ leader sequence acts to promote cap-independent translation. The RNA of plant potyviruses (which includes TEV) have a 5′ VPg (viral protein genome linked)[19]. Further, this RNA is also polyadenylated. The TEV viral RNA 5′ VPg is removed prior to recruitment of the mRNA into polysomes and it has been shown that the 5′ IRES is sufficient to confer cap-independent translation [20–22].

1.1 5′ IRES

Internal ribosome entry sites have been known and studied for some time. Perhaps two of the earliest and most studied are those from encephalomyocarditis and polio virus. For encephalomyocarditis virus and poliovirus the leader sequences are 1,300 and 650 nt in length [13]. These sequences are highly structured and contain multiple AUGs upstream of the initiation codon. Initiation factors eIF3 and eIF4G bind to segments of the IRES and recruit 40S ribosomal subunits for internal initiation [23].

For plants, those viral mRNAs that lack a cap must also follow cap-independent translation. Tobacco mosaic virus leader sequence has been extensively investigated as a translational enhancer [24–27]. The tobacco mosaic virus 5′ leader sequence (called omega) requires eIF4F and eIF3 for translational enhancement [14]. The TEV 5′ UTR is 143 nt in length and is one of the smallest viral elements identified that can promote cap-independent translation. Two regions within the UTR were identified as necessary to direct cap-independent translation, and their combined effect was approximately multiplicative, suggesting the two elements are part of a single regulatory region [28]. Recently [16], chemical probing and mutational analysis showed that the 143-nt leader folds into two domains, each of which contains a pseudoknot. The proposed folding of the leader sequence is shown in Fig. 1.

Gallie's detailed chemical probing, mutational analysis and translational assays identified PK1 and a single-stranded region flanking PK1 as necessary to promote cap-independent translation. Mutations to either stem or loop 2 or 3 of PK1 substantially reduced translation of a luciferase reporter gene. Loop 3 contains a sequence complementary to 18S ribosomal RNA, and mutations that disrupt this potential base pairing also change translational activity.

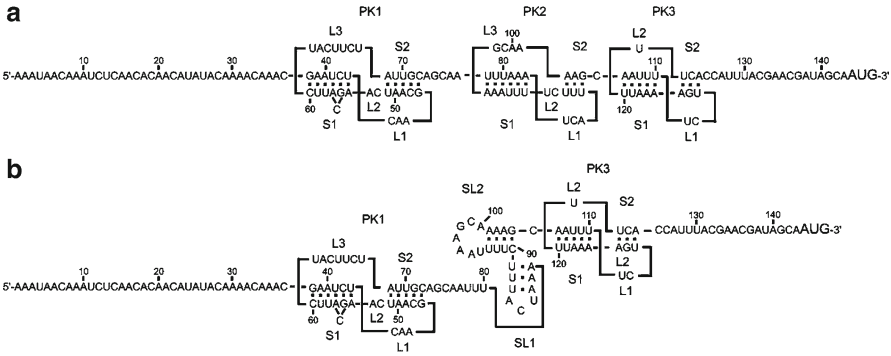

Fig. 1 Predicted structure of TEV 5′ leader (from Zeenko and Gallie [16])

1.2 Initiation Factor Requirements

Both plants and animals have been shown to have two eIF4G proteins [29–32]. In plants these are designated eIF4G and eIFiso4G (165 and 86 kDa, respectively) and have 30% consensus identity (unpublished data quoted in Gallie and Browning [33]). EIF4G was shown to be necessary for cap-independent translation of TEV mRNA [14] and has been shown to be functionally different from eIFiso4G in promoting internal initiation and translation of structured RNA [33].

2 Fluorescence Studies

2.1 Specificity of Binding

Functional studies showed that in vitro translation using the 5′ TEV leader to direct cap-independent translation required eIF4G and not eIFiso4G. In order to determine if these results were the result of direct binding affinity, we determined the binding of both proteins to TEV RNA directly. The problem with determining binding of a relatively large oligonucleotide is that if fluorescence quenching is used, there is absorbance from the RNA and if labeling of the RNA is used, it is likely that the label (usually 5′ or 3′) is so far from the binding site that it may not report binding. In order to overcome the first of these problems, we used quenching of intrinsic protein fluorescence and corrected for inner filter effects using *N*-acetyltryptophanamide (NATA) as a standard [15, 34]. The observed fluorescence intensity of 10 μM NATA was monitored at 333 nm exciting at 280 nm for each concentration of TEV RNA. The absorbance of each TEV RNA concentration was measured at 280 nm. The fluorescence intensity of NATA was normalized and plotted against the absorption of TEV RNA (Fig. 2a). Normalized NATA data vs. RNA concentration was generated

by fitting with a first-order exponential decay. The normalized NATA corrections to the observed intensities were calculated using:

$$F_{\text{corr}} = \frac{F_{\text{obs}}}{C_{\text{f}}}$$

where F_{corr} and F_{obs} are the corrected and observed fluorescence intensities, respectively, and C_{f} is the NATA correction factor. Inner filter corrections were also applied.

The dissociation equilibrium constants for the protein–TEV RNA binding were determined from nonlinear curve fitting. ΔF_{max}, the fluorescence change for complete saturation of the protein with ligand, was determined from a double-reciprocal plot, which was also used to determine K_{a}, the association binding constant. K_{a} is, of course, equal to $1/K_{\text{d}}$ so that this additional fitting is a check on the consistency of the nonlinear fitting. The equation used was:

$$\frac{1}{\Delta F} = \frac{1}{\Delta F_{\text{max}}} + \frac{1}{\left[K_{\text{a}} \Delta F_{\text{max}} \left(C_{\text{L}} - C_0\right)\right]}$$

C_{L} is the concentration of the RNA and C_0 is the initial concentration of protein. The linear plot of $1/\Delta F$ against $1/(C_{\text{L}} - C_0)$ is extrapolated to obtain ΔF_{max} from the intercept. The double-reciprocal plot is shown in the inset of Fig. 2b. This approach is based on the assumption that the emission intensity is proportional to the concentration of the ligand and $C_{\text{L}} >> C_0$, i.e. when RNA concentration is in excess compared to protein concentration.

A comparison of binding affinity of the two isoforms, eIF4G and eIFiso4G, demonstrated that eIF4G bound TEV RNA with ~30-fold stronger affinity than eIFiso4G. Control studies of binding to a mutant of the TEV IRES showed that this binding was specific [15]. Temperature dependence of the equilibrium constants gave thermodynamic parameters, ΔH and ΔS. These studies showed protein binding had a large entropic contribution, suggesting that binding may be influenced by hydrophobic interactions. These results demonstrate the interaction of eIF4G with the TEV IRES in the absence of other eIFs and correlate well with the observed translational data.

2.2 Multi-protein Binding to TEV RNA

Translation of IRES RNA may involve a number of protein factors (for a review see [1]). In order to determine the effects of multiple factors, e.g. cooperative or competitive interactions, we have measured the binding affinity of a number of eIF complexes with TEV RNA [15, 35, 36]. In order to accurately measure the binding

constants, we have determined the protein–protein interactions and the individual protein interactions with TEV RNA. The protein–protein K_ds are necessary to determine the concentration of proteins required to ensure that the binding protein is actually in a complex with the other factors. For example, if we want to measure the effect of PABP on eIF4F binding, we need to be sure most of the eIF4F is in a complex with PABP. We also need to know the binding affinity of PABP for TEV RNA alone. In this example, the experiment is straightforward because PABP has very low binding affinity for TEV 5′ RNA. Therefore, we used an excess of PABP to eIF4F in order to form the PABP-eIF4F complex and measured binding to fluorescein labeled TEV PK1 RNA by monitoring changes in fluorescence anisotropy. PABP is necessary for the formation of the 48S initiation complex and interaction of PABP with eIFiso4F was shown to enhance cap-binding by about 40-fold [5]. We were curious to see if PABP would have a similar effect on enhancing binding to the internal TEV initiation site.

The anisotropy was measured for each sample using an excitation wavelength of 490 nm and emission of 519 nm. At these wavelengths, corrections for absorbance or inner filter effects are not necessary. The anisotropy data was fitted to the following equation [37, 38]:

$$r_{obs} = r_{min} + \left\{ \frac{r_{max} - r_{min}}{2\,[^{Fl}PK1]} \right\} \left\{ b - (b^2 - 4[^{Fl}PK1][elF])^{0.5} \right\}$$

where $b = K_d + [^{Fl}PK1] + [eIFs]$, r_{obs} is the observed anisotropy for any point in the titration curve, r_{min} is the minimum observed anisotropy in the absence of protein, r_{max} is the maximum anisotropy at saturation and is fit as a parameter. $[^{Fl}PK1]$ and [eIFs] are the PK1 RNA and protein concentrations. K_d is the equilibrium dissociation constant.

Protein–protein interactions were monitored by changes in intrinsic protein fluorescence (complex fluorescence-sum of individual proteins) and these K_d values [36] were used to calculate the amount of protein necessary to have 90% of the eIF4F in a protein complex at 50 nM, the lowest protein titration point. For eIF4F-PABP, this was a 1:10 molar ratio. Binding curves for TEV RNA are shown in Fig. 3 below (from Khan et al. [36]).

While PABP does enhance binding of eIF4F to the IRES, it clearly does not stimulate binding to the same extent as it does for cap-binding.

Temperature-dependent studies of these equilibria allowed determination of thermodynamic parameters to show enthalpic and entropic contributions from van't Hoff plots (ln K_{eq} vs. $1/T$). As mentioned above, eIF4F binding to TEV RNA has a large entropic contribution which suggests hydrophobic interactions. The addition of eIF4B to the eIF4F had little effect on the enthalpic or entropic parameters, however, addition of both eIF4B and PABP reduced the entropic contribution from 59% for eIF4F alone to about 20% at 25°C [36]. One interpretation of these data is that the protein–protein interactions are largely hydrophobic, while the protein complexes interact with RNA through hydrogen bonds.

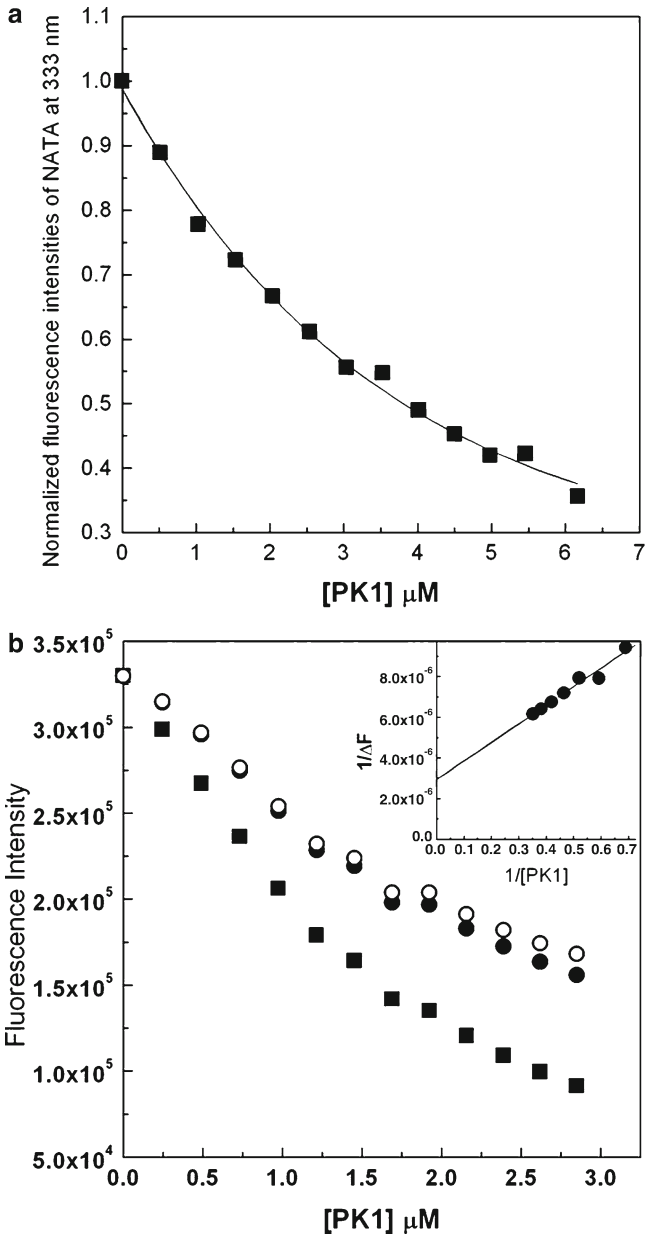

Fig. 2 A fluorescence quenching of eIFiso4G titrated with PK1. (**a**) fluorescence quenching of NATA (10 μM) titrated with PK1 RNA. Normalized data of 10 μM NATA (*filled square*) were used to correct binding data. (**b**) Fluorescence quenching, inner filter corrected, and NATA corrected plots of eIFiso4G (0.2 μM), titrated with PK1. The observed (*filled square*), NATA corrected (*filled circle*), and inner filter corrected (*open circle*) fluorescence emission intensities of eIFiso4G vs. PK1 RNA concentration are shown. The excitation wavelength was 280 nm and emission intensities were measured at 333 nm at 25°C. The *inset* is a double-reciprocal plot of $1/\Delta F$ vs. 1/[PK1] for eIFiso4G (0.2 μM) [15]

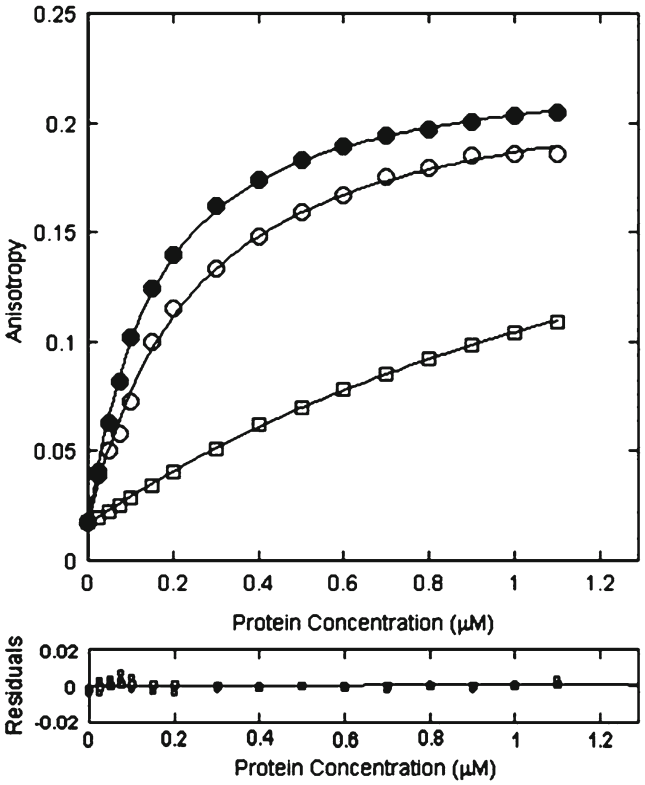

Fig. 3 Fluorescence anisotropy measurements for the binding of PK1 (^{Fl}PK1) RNA with translation initiation factors. The anisotropy values of eIF4F–PK1 (—○—), eIF4F·PABP–PK1 (—●—) and PABP-PK1 (—□—) are shown. The fluorescein PK1 RNA concentration was 50 nM in titration buffer at 25°C. The excitation and emission wavelengths were 490 nm and 519 nm, respectively. The curves were fit to obtain dissociation constants (K_d) as described. The solid lines are the fitted curves. eIF4F·PABP (1:10) complex was prepared by incubation of 1 μM eIF4F and 10 μM PABP for 15 min at 4°C, and 91% of the protein sample was in complex form at 50-nM titration concentration. Residuals for the fits are shown in the lower panels. From Khan et al. [43]

For eIF4F-PK1 the enthalpy was -15.1 ± 1.5 kJ mol^{-1} and the entropy was 76 ± 3.6 J mol^{-1} K^{-1}, in contrast to cap-binding where the values were 28.7 ± 0.7 kJ mol^{-1} and 199 ± 5 J mol^{-1} K^{-1} for enthalpy and entropy, respectively [15]. These large differences in the thermodynamic parameters suggest significant differences in the mode of binding. It is not surprising that cap binding is entropically driven given the large conformational change that occurs in the eIF4E subunit. The fact that eIF4F binding to TEV RNA, especially in combination with eIF4B and PABP, is not entropically driven and also has a favorable enthalpic contribution suggests that conformational changes, especially in eIF4G, play a smaller role in complex stability. Overall, these equilibrium data show that eIF4F complex binds to

TEV RNA with greater stability than the cap complex. This stability will favor ribosome binding, but additional factors are also likely to play into the competition for initiation complex formation. Since cap binding is thought to be the rate-limiting step for protein synthesis initiation, viral RNA may have a kinetic advantage over host cell RNA. Selective translation can be achieved by increased stability of the initiation complex to provide a better "landing pad" for ribosomes, or eIFs can simply bind faster to the viral RNA so that a larger percentage of viral RNA is primed for translation. To further understand the assembly process, we have examined the kinetics of eIFs binding to TEV RNA.

2.3 Kinetics of eIF Binding to TEV RNA

Kinetic parameters can not only give information about how fast TEV RNA can compete with host cell RNA for eIFs, but concentration dependence and ionic strength dependence of the reactions can provide mechanistic information about the association. Because eIF4F equilibrium binding to TEV RNA is only moderately stronger than cap binding, we wondered if the kinetics of the process could further explain the translational advantage of TEV RNA and provide insight into the binding mechanism.

Stopped-flow anisotropy measurements were used to monitor eIF4F and eIF4F-eIF4B-PABP complex binding to TEV RNA, which was fluorescently labeled with fluorescein at the 5′ terminus [39]. To distinguish between a single, bimolecular binding mechanism and more complex mechanisms, data were fit with a single and double exponential function and the concentration dependence of the reactions were measured. For a simple one-step reaction mechanism shown below:

$$\mathrm{eIF4F} + \mathrm{PK1} \underset{k_{\mathrm{off}}}{\overset{k_{\mathrm{on}}}{\rightleftharpoons}} \mathrm{eIF4F-PK1}$$

Mechanism 1

where k_{on} and k_{off} are the rates of association and dissociation, respectively, the observed rate constant, k_{obs}, is predicted to be a linear function of eIF4F concentration since [eIF4F] is in excess:

$$k_{\mathrm{obs}} = k_{\mathrm{on}}\left[\mathrm{eIF4F}\right] + k_{\mathrm{off}}$$

For a more complex mechanism where the initial binding is followed by a conformational change that is rate-limiting as shown below:

$$\mathrm{eIF4F} + \mathrm{PK1} \underset{k_{-1}}{\overset{k_{1}}{\rightleftharpoons}} \mathrm{eIF4F \cdot PK1^{*}} \underset{k_{-2}}{\overset{k_{2}}{\rightleftharpoons}} \mathrm{eIF4F \cdot PK1}$$

where the first step is the bimolecular association to form an intermediate (eIF4F·PK1*) and the second step represents a conformational change to achieve the final, stable product. For this mechanism [40], if one assumes that $k_{-2} << k_{obs}$, then:

$$\frac{1}{k_{obs}} = \frac{1}{k_2} + \frac{k_1}{k_2 \left[\text{eIF4F}\right]}$$

and a plot of $1/k_{obs}$ vs. 1/[eIF4F] will be linear.

Figure 4 shows the linear concentration dependence for eIF4F binding to PK1 RNA, demonstrating that the experimental results are consistent with a bimolecular, single-step reaction. However, the ionic strength dependence of the reaction revealed a more complex mechanism for binding. The association rate was reduced more than tenfold when the KCl concentration was increased from 50 to 300 mM, but the dissociation rate was increased only twofold. The fact that the ionic strength dependence of the "on" and "off" rates are different suggests that electrostatic interactions are more important for the "on" rate than for the dissociation rate. A possible explanation for this is that the initial interaction of eIF4F or the protein complex with PK1 is electrostatic in nature. A subsequent conformational change then occurs to form the final stable complex. Such a mechanism will have a larger electrostatic (ionic strength dependence) for the association rate and a correspondingly smaller electrostatic component to the dissociation rate.

One strategy a virus might employ to give a competitive advantage to translation of its own RNA is to have more rapid binding to the viral RNA compared to host cell RNA. We therefore compared binding of eIF complexes to TEV RNA and capped oligonucleotides. Kinetics showed similar binding mechanisms for both TEV and capped oligonucleotides. The capped RNA showed a lower k_{on} and nearly identical k_{off} values. Although TEV RNA does not possess a large kinetic advantage, the eIF complex will partition to the TEV RNA when viral and host cell RNA are in similar concentrations. The faster association rates for TEV binding will allow a greater opportunity for ribosome binding.

3 Discussion

Gallie [14] has shown that in vitro, when eIF4F is limiting, TEV is preferentially translated and under their experimental conditions the level of TEV-luc-A_{50} was 90-fold greater than a control mRNA. The association rate constants are very similar for capped and uncapped RNA [39], which would partition about half of the eIF4F to the TEV RNA if the concentrations of TEV RNA and control mRNA are equal. At the early stages of infection, the viral RNA is probably in much lower concentrations than host cell mRNA. However, the equilibrium data, which show that eIF4F bound TEV RNA 15–20 more tightly than capped oligonucleotide, suggest a slow dissociation rate and effectively a sequestering of the eIF4F to the viral RNA. The effects of PABP and eIF4B on cap binding are to decrease the dissociation rate; however, for viral RNA the effects are to increase the association rates. The influence

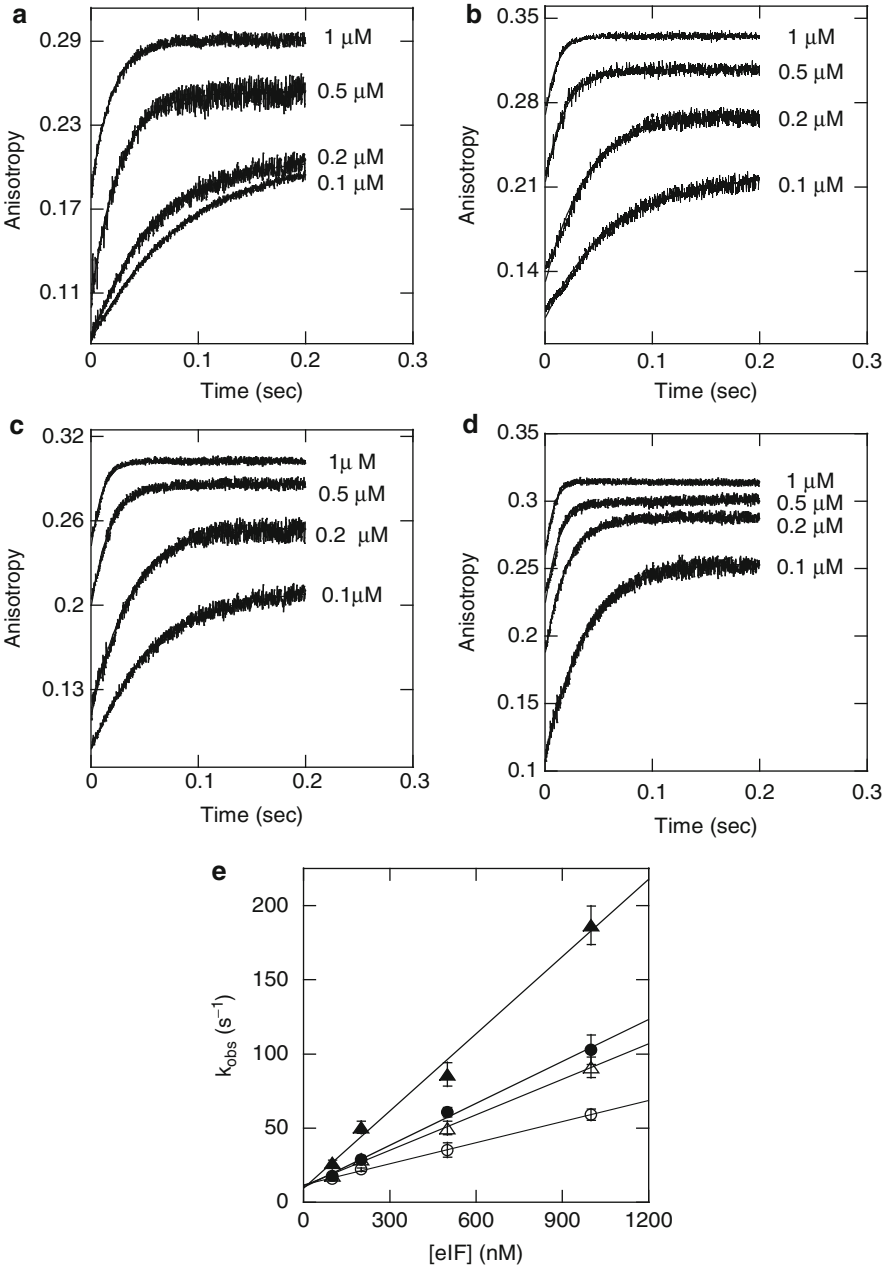

Fig. 4 Initiation factor binding to PK1 RNA is linearly dependent on concentration. ^{Fl}PK1 RNA at 50 nM (final) was rapidly mixed with varying concentrations (0.1, 0.2, 0.5 and 1 μM, final) of (**a**) eIF4F, (**b**) eIF4F·4B, (**c**) eIF4F·PABP, and (**d**) eIF4F·4B·PABP. The *solid line* represents the fitted curve for a single-exponential function. (**e**) The observed rate constant for the anisotropy change is plotted as a function of increasing concentrations of eIF4F (—○—), eIF4F·4B (—●—), eIF4F·PABP (—Δ—), and eIF4F·4B·PABP (—▲—). The linear concentration dependence suggests a simple second order reaction (adapted from Khan et al. [39])

of PABP and eIF4B on equilibrium and binding rates suggest that the most productive IRES recruitment would occur subsequent to protein complex formation. This suggests a model where subsequent to viral RNA entering the cell, the protein complex binds to the IRES-RNA. Earlier studies [35, 41] showed that the viral protein, VPg, can compete with cap for eIF4F binding. VPg can displace the protein complex from mRNA and free the complex to bind to IRES-RNA. However, there may be other reasons or mechanisms for TEV IRES competition with host mRNA. Additional initiation factors and poly A may increase the rate of binding to viral RNA. It has not been determined whether helicase reactions play a role in viral translation, either through eIF4F binding or ribosome binding. The TEV IRES, like other IRES contains secondary structure, but the extent to which this secondary structure is unwound or modified during translation is for the most part unknown. Further, recruitment of eIF4F to the TEV IRES may be enhanced by other trans-acting factor(s), which are increasingly being discovered, such as ITAF45 protein for foot-and-mouth disease virus [42]. Identification of other proteins and the dynamics of RNA structural motifs will be necessary to fully determine the translational strategy of TEV and other members of this family.

Acknowledgments This work was supported by NSF grant MCB 0814051. The author wishes to thank the many members of her research group who contributed to these studies, in particular Dr. Mateen Khan, Hasan Yumak, Shemaila Sultana, Sibnath Ray, Artem Domashevskiy, Sumeyra Yumak and Dr. John Trujillo.

References

1. Fitzgerald K, Semler B (2009) Bridging IRES elements in mRNAs to the eukaryotic translation apparatus. Biochim Biophys Acta 1789:518–528
2. Pestova T, Kolupaeva V, Lomakin I, Pilipenko E, Shatsky I, Agol V, Hellen C (2001) Molecular mechanisms of translation initiation in eukaryotes. Proc Natl Acad Sci USA 98:7029–7036
3. Sonenberg N, Dever TE (2003) Eukaryotic translation initiation factors and regulators. Curr Opin Struct Biol 13:56–63
4. Le H, Tanguay RL, Balasta ML, Wei C-C, Browning KS, Metz AM, Goss DJ, Gallie DR (1997) The translation initiation factors eIF-iso4G and eIF4B interact with the poly(A)-binding protein and increase its RNA binding affinity. J Biol Chem 272:16247–16255
5. Wei C-C, Balasta ML, Ren J, Goss DJ (1998) Wheat germ poly(A) binding protein enhances the binding affinity of eukaryotic initiation factor 4F and (iso)4F for cap analogs. Biochemistry 37:1910–1916
6. Hellen CUT, Sarnow P (2001) Internal ribosome entry sites in eukaryotic mRNA molecules. Genes Dev 15:1593–1612
7. Kean KM (2003) The role of mRNA 5′-noncoding and 3′-end sequences on 40S ribosomal subunit recruitment, and how RNA viruses successfully compete with cellular mRNAs to ensure their own protein synthesis. Biol Cell 95:129–139
8. Jang S, Krausslich H-G, Nicklin M, Duke G, Palmenberg A, Wimmer E (1988) A segment of the 5′ nontranslated region of encephalomyocarditis virus RNA directs internal entry of ribosomes during in vitro translation. J Virol 62:2636–2643
9. Pelletier J, Sonenberg N (1988) Internal initiation of translation of eukaryotic mRNA directed by a sequence derived from poliovirus RNA. Nature 334:320–325

10. Pestova T, Hellen C, Shatsky I (1996) Canonical eukaryotic initiation factors determine initiation of translation by internal ribosomal entry. Mol Cell Biol 16:6859–6869
11. Carrington J, Freed D (1990) Cap-independent enhancement of translation by a plant potyvirus 5′ nontranslated region. J Virol 64:1590–1597
12. Gallie D, Tanguay R, Leathers V (1995) The tobacco etch viral 5′ leader and poly(A) tail are synergistic regulators of translation. Gene 165:233–238
13. Palmenberg A (1987) Comparative organization and genome structure in picornaviruses. UCLS Symp Mol Cell Biol 54:25–34
14. Gallie D (2001) Cap-Independent translation conferred by the 5′ leader of tobacco etch virus is eukaryotic initiation factor 4G dependent. J Virol 75:12141–12152
15. Ray S, Yumak H, Domashevskiy A, Khan M, Gallie DR, Goss DJ (2006) Tobacco etch virus mRNA preferentially binds wheat germ eukaryotic initiation factor (eIF)4G rather than eIFiso4G. J Biol Chem 281:35826–35834
16. Zeenko V, Gallie DR (2005) Cap-independent translation of tobacco etch virus is conferred by an RNA pseudoknot in the 5′-leader. J Biol Chem 280:26813–26824
17. Thivierge K, Nicaise V, Dufresne P, Cotton S, Laliberte J-F, Le Gall O, Fortin M (2005) Plant virus RNAs. Coordinated recruitment of conserved host functions by (+) ssRNA viruses during early infection events. Plant Physiol 138:1822–1827
18. Mohr I (2006) Phosphorylation and dephosphorylation events that regulate viral mRNA translation. Virus Res 119:89–99
19. Dougherty W, Carrington J (1988) Expression and function of potyviral gene products. Ann Rev Phytopathol 26:123–143
20. Pettersson R, Flanegan J, Rose J, Baltimore D (1977) 5′-terminal nucleotide sequences of polio virus polyribosomal RNA and virion RNA are identical. Nature 268:270–272
21. Nomoto A, Kitamura N, Golini F, Wimmer E (1977) The 5′-terminal structures of poliovirion RNA and poliovirus mRNA differ only in the genom-linked protein VPg. Proc Natl Acad Sci USA 73:5345–5349
22. Hewlett M, Rose J, Baltimore D (1976) 5′-terminal structure of poliovirus polyribosomal RNA is pUp. Proc Natl Acad Sci USA 73:327–330
23. Ehrenfeld E (1996) Initiation of translation by picornavirus RNAs. Translational control. Cold Spring Harbor, New York, pp 549–574
24. Gallie D, Walbot V (1992) Identification of the motifs within the tobacco mosaic virus 5′ leader responsible for enhancing translation. Nucleic Acids Res 20:4631–4638
25. Gallie D (2002) The 5′-leader of tobacco mosaic virus promotes translation through enhanced recruitment of eIF4F. Nucleic Acids Res 30:3401–3411
26. Gallie D, Sleat D, Watts J, Turner PC, Wilson TM (1987) The 5′-leader sequence of tobacco mosaic virus RNA enhances the expression of foreign gene transcripts in vitro and in vivo. Nucleic Acids Res 15:3257–3273
27. Gallie D, Sleat D, Watts J, Turner P, Wilson T (1988) Mutational analysis of the tobacco mosaic virus 5′-leader for altered ability to enhance translation. Nucleic Acids Res 16:883–893
28. Niepel M, Gallie D (1999) Identification and characterization of the functional elements within the tobacco etch virus 5′ leader required for cap-independent translation. J Virol 73: 9080–9088
29. Goyer C, Altmann M, Lee H, Blanc A, Deshmukh M, Woolford J Jr, Trachsel H, Sonenberg N (1993) TIF4631 and TIF4632: two yeast genes encoding the high-molecular-weight subunits of the cap-binding protein complex (eukaryotic initiation factor 4F) contain an RNA recognition motif-like sequence and carry out an essential function. Mol Cell Biol 13:4860–4874
30. Gradi A, Svitkin Y, Imataka H, Sonenberg N (1998) Proteolysis of human eukaryotic translation initiation factor eIF4GII, but not eIF4GI, coincides with the shutoff of host protein synthesis after poliovirus infection. Proc Natl Acad Sci USA 95:11089–11094
31. Browning KS (1996) The plant translational apparatus. Plant Mol Biol 32:107–144
32. Imataka H, Gradi A, Sonenberg N (1998) A newly identified N-terminal amino acid sequence of human eIF4G binds poly(a)-binding protein and functions in poly(A)-dependent translation. EMBO J 17:7480–7489

33. Gallie DR, Browning K (2001) EIF4G functionally differs from eIFiso4G in promoting internal initiation, cap-independent translation, and translation of structured mRNAs. J Biol Chem 276:36915–36960
34. Rambo R, Doudna J (2004) Biochemistry 44:4510–4516
35. Khan M, Miyoshi H, Gallie DR, Goss DJ (2008) Potyvirus genome-linked protein, VPg, directly affects wheat germ in vitro translation: interactions with translation initiation factors eIF4F and eIFiso4F. J Biol Chem 283:1340–1349
36. Khan MA, Yumak H, Gallie DR, Goss DJ (2008) Effects of poly(A)-binding protein on the interactions of translation initiation factor eIF4F and eIF4F-4B with internal ribosome entry site (IRES) of tobacco etch virus RNA. Biochim Biophys Acta 1779:622–627
37. Kohler J, Schepartz A (2001) Kinetic studies of Fos, Jun DNA complex formation: DNA binding prior to dimerization. Biochemistry 40:130–142
38. Tayyab S, Khan N, Khan MA, Kumar Y (2003) Behavior of various mammalian albumins towards bilirubin binding and photochemical properties of different bilirubin–albumin complexes. Int J Biol Macromol 31:187–193
39. Khan MA, Yumak H, Goss DJ (2009) Kinetic mechanism for the binding of eIF4F and tobacco etch virus internal ribosome entry site RNA: effects of eIF4B and Poly(A)-binding protein. J Biol Chem 284:35461–35470
40. Sha M, Wang Y, Xiang T, van Heerden A, Browning K, Goss DJ (1995) Interaction of wheat germ protein synthesis initiation factor eIF-(iso)4F and its subunits p28 and p86 with m7GTP and mRNA analogs. J Biol Chem 270:29904–29909
41. Khan M, Miyoshi H, Ray S, Natsuaki T, Suehiro N, Goss DJ (2006) Interaction of genome-linked protein (VPg) of turnip mosaic virus with wheat germ translation initiation factors eIFiso4E and eIFiso4F. J Biol Chem 281:2802–2810
42. Pilipenko E, Pestova T, Kolupaeva V, Khitrina E, Poperechnaya A, Agol V, Hellen C (2000) A cell cycle-dependent protein serves as a template-specific translation initiation factor. Genes Dev 14:2028–2045
43. Khan MA, Goss DJ (2005) Translation initiation factor (eIF) 4B affects the rates of binding of the mRNA m7G cap analogue to wheat germ eIFiso4F and eIFiso4F-PABP. Biochemistry 44:4510–4516

Novel Metal-Based Luminophores for Biological Imaging

David Lloyd, Michael P. Coogan, and Simon J.A. Pope

Abstract This review aims to summarise key recent developments regarding the use of luminescent metal complexes in biological imaging. The photophysical advantages of *d*- and *f*-block complexes are discussed and specific examples of cellular imaging are described through confocal fluorescence microscopy studies. Issues of complex design and specific organelle targeting are considered together with the use of a phosphorescent ruthenium complex to monitor intracellular oxygen levels in real-time, via microscopy and time-resolved luminescence methods. The development of near-IR-emissive probes based on lanthanide complexes are also briefly presented, together with strategies for their application as responsive reporters in a biological context.

1 Introduction

The use of biological imaging is central to the elucidation of key questions in the continuing search for molecular mechanisms that underpin biomedical, veterinary, agricultural and industrial problems. Such problems often necessitate novel probes with exploitable luminescent properties. Luminescent metal coordination complexes are increasingly seen as attractive candidates for such tasks due to their dual applicability to (a) optical imaging and (b) targeted molecular probes. Those based

D. Lloyd (✉)
Department of Microbiology, Cardiff Schools of Bioscience, Cardiff University, Main Building, Museum Avenue, Cathays Park, Cardiff CF10 3AT, Wales, UK
e-mail: lloydd@cardiff.ac.uk

M.P. Coogan • S.J.A. Pope
Cardiff School of Chemistry, Cardiff University, Main Building, Museum Avenue, Cathays Park, Cardiff CF10 3AT, Wales, UK

C.D. Geddes (ed.), *Reviews in Fluorescence 2010*,
Reviews in Fluorescence, DOI 10.1007/978-1-4419-9828-6_2,

upon either platinum-group or lanthanide-series metal ions have many desirable and wide-ranging properties for such applications. These can include:

- Tunable emission throughout the visible and near-IR regions
- Long luminescence lifetimes (from hundreds of nanosecond to millisecond domain)
- Good luminescence quantum yields, sometimes exceeding 0.5
- Large Stokes shifts (often >5,000 cm^{-1})
- Good thermal, chemical and photochemical stability and metabolic inertness [1–9]

Biological criteria for the ideal luminescent probe include: (a) rapid penetration of the compound into the cell; (b) uniform distribution within the highly structured and compartmentalised cellular ultrastructure; (c) well-defined characteristics of alterations in absorption and emission (absorption coefficients and quantum yields) that may result from binding to cellular molecular constituents or membranes; (d) the presence of probe should be without metabolic effects and (e) for long-term monitoring, they should not influence either survival or the capacity for cellular growth and reproduction.

The application of late-transition metal complexes, and especially polypyridyl complexes, in biological imaging has been the focus of a great deal of interest with d^6-transition metal complexes, such as Re^{I} [2–4], Ru^{II} [5] and Ir^{III} [6] in particular, showing useful application in cellular imaging studies. The emissive lanthanide ions also offer additional opportunities for luminophore design and application. For example, complexes of Eu(III), Tb(III) and Sm(III) offer visible luminescence [10], whereas Nd(III), Er(III) and Yb(III) possess low-energy emission extending well into the near-IR region [11]. In all cases, the nature of the lanthanide-based emission differs fundamentally from those *d*-metal complexes discussed above, originating from 4*f*-(metal) centred excited states. Relaxation from these excited states is formally forbidden, resulting therefore in very long emission lifetimes that typically range from millisecond (Eu and Tb) through microseconds (Yb(III)) to nanoseconds (Nd(III)) domains. Cellular imaging with visibly emissive Ln(III) complexes is now established utilising both macrocyclic [7] and helical bimetallic complexes [8], but further development towards deeper tissue imaging requires the use of low-energy wavelengths (i.e. near IR) since biological tissue possesses a much greater transparency to near-IR wavelengths in comparison to visible and UV wavelengths. In this regard, Ln(III) complexes again have much to offer since Nd(III), Pr(III), Er(III) and Yb(III) are all emissive in the near-IR region, and as the technology of sensitive, near-IR detection improves complexes based on these ions may be extremely useful in optical imaging applications involving confocal fluorescence and lifetime imaging microscopy.

2 Development and Application of Novel d^6-Transition Metal Luminophores

Luminescent d^6 complexes of Ir(III) [12], Re(I) [13] and Ru(II) [14] with polypyridyl or organometallic ligands are attractive for application in imaging due to common characteristics, including the kinetic inertness of low spin d^6 octahedral

complexes, which is important to prevent ligand substitution and associated toxicity and for air and water stability; large Stokes shifts (>100 nm); long luminescence lifetimes (hundreds of ns to μs) and high photostability (low photobleaching). In order to overcome problems associated with membrane permeability and uptake, some groups have chosen to conjugate such complexes to biomolecules [4, 5] or incorporate lipophilic entities into their complexes [6]. Ir and Ru are promising candidates for these applications, but Re has particular features, which make it an attractive candidate, in that the excited state is localised on a single ligand, allowing a degree of tuning in the emission characteristics, and the axial (usually, a pyridine) ligand therefore allows a photophysically innocent point for attachment of, e.g. lipophilic groups to assist the uptake.

2.1 Rhenium Complexes in Sensing Applications

Rhenium complexes have been applied as chemosensors or probes for molecules and ions and, in particular, cationic rhenium complexes have been proposed as anion sensors [15]. Rhenium ^{3}MLCT emission can also be sensitive to the presence of dissolved dioxygen and rhenium complexes have also been shown to be capable of indicating oxygen levels by luminescence lifetime [16], although none have been applied in cellular oxygen mapping. DeGraff and Demas [17] used the protection of the excited state of rhenium complexes in macromolecules to show responses to cyclodextrins through host–guest interactions.

A rhenium complex functionalised with an alkyl chain has been developed as a probe for the local environment through a hydrophobically driven chain-wrapping mechanism inducing lengthening of the excited state lifetime in water. However, in the presence of proteins containing a fatty acid-binding pocket or lipid membranes, the alkyl chain is extended leaving the excited state exposed to solvent, resulting in a shorter lifetime [3, 18].

In a rare example of cation sensing, encapsulation of a silver ion in a neutral luminescent rhenium macrocyclic ligand changes the system's emissivity giving a prototype metal-ion sensor [19]. Responsive, luminescent lifetime probes based upon axially functionalised fac-$[Re(CO)_3$(di-imine)(L)$]^+$ complexes have also been prepared, where axial ligand, L, incorporates a binding site targeted towards metal cations of physiological and toxicological importance (Cu^{2+}, Zn^{2+} and Hg^{2+}). Cation binding in acetonitrile results in modulation of emission profiles and ^{3}MLCT lifetimes and the latter parameter can be exploited to discriminate between analytes in an ionic background [20].

2.2 Rhenium Complexes in Cell Imaging Applications

The first report of a rhenium complex in fluorescent cell imaging [21] was of bisquinoline complexes conjugated to fMLF, a peptide previously used [22] in radioimaging